VLT observations of Fermi pulsars

R. P. Mignani[1,2], A. Shearer[3], A. De Luca[4,5,6], P. Moran[3], S. Collins[3], M. Marelli[5,7], D.A. Smith[8,9]

[1]Mullard Space Science Laboratory, University College London, UK; [2]Institute of Astronomy, University of Zielona Gora, Poland;; [3]Centre for Astronomy, National University of Ireland, Ireland; [4]Istituto Universitario di Studi Superiori, Pavia, Italy; [5]Istituto di Astrofisica Spaziale e Fisica Cosmica Milano, Italy; [6]Istituto Nazionale di Fisica Nucleare, sezione di Pavia, Italy; [7]Universita' degli Studi dell' Insubria, Varese, Italy, [8]Universite' de Bordeaux, Centre d'etudes nucleaires de Bordeaux , Gradignan, France ; [9] CNRS/IN2P3, Centre d''' etudes nucleaires de Bordeaux, France

Abstract

Many energetic γ-ray pulsars discovered by Fermi are promising candidates for optical follow-ups. We present the results of the first deep optical observations of the two Vela-like Fermi pulsars PSR J1357−6429 and PSR J1048−5832 performed with the VLT. However, they have not been detected down to V~27 and V~28, respectively (3σ). These upper limits suggest an efficiency in converting spin-down power into optical luminosity $<10^{-7}$ and $<10^{-6}$, respectively, lower than the Crab pulsar and, possibly, more compatible with the spin-down age of these two pulsars.

Introduction

Optical observations of pulsars are crucial to study the intrinsic properties of neutron stars, from the structure and composition of the interior, to the properties and geometry of the magnetosphere. Historically, X-ray and γ-ray observations have paved the way to the pulsar optical identifications, with all the presently identified pulsars also detected at high energies (see, Mignani 2011 for a recent review). In particular, 5 out of the 7 γ-ray pulsars detected by NASA's CGRO satellite have also been detected in the optical, suggesting that γ-ray detections highlight promising candidates for optical observations, since the emission at both energies seems to correlate with the strength of the magnetic field at the light cylinder (Shearer & Golden 2001; Shearer et al. 2010).The launch of the Fermi Gamma-ray Space Telescope opened new perspectives with the detection of over 60 γ-ray pulsars by the Large Area Telescope (LAT). For most Fermi pulsars, however, no deep optical observations have been carried out so far. A survey in the Northern hemisphere has been carried out with 2.5m/4m telescopes at the La Palma Observatory but no pulsar has been detected (Shearer et al. 2011 – see also poster by Shearer et al.), while in the Southern hemisphere a survey with the VLT is in progress (see Mignani et al., 2011a for early results).

Here, we present the search for the optical counterparts of two Fermi pulsars, which are potentially interesting targets on the basis of their spin-down age, energetics, and distance (Mignani et al. 2011b). PSR J1357−6429 is a very young (7.31 kyr old) pulsar (P = 166.1 ms), at a distance of ~2.5 kpc, with a rotational energy loss rate $dE/dt \sim 3\times10^{36}$ erg s^{-1}. It has possibly been detected as a gamma-ray pulsar also by AGILE and its associated pulsar wind nebula (PWN) has been detected at TeV energies by HESS. PSR J1048−5832 is a 20.3 kyr old, Vela-like, pulsars (P=123.6 ms), tentatively detected by the CGRO, at a distance of ~2.7 kpc and with a $dE/dt \sim 2\times10^{36}$ erg s^{-1} comparable to that of PSR J1357−6429. Both pulsars are also detected in X-rays by both XMM-Newton and Chandra. No deep optical observations of these two pulsars have been ever reported. We used multi-band images (V, R, I) taken with the VLT and available in the ESO public archive to search for, or put tight constraints to, their optical emission.

Observations

Optical images of the PSR J1357−6429 and PSR J1048−5832 fields were obtained with the VLT between April 2009 and February 2010. Observations were performed in service mode with FORS2, a multi-mode camera for imaging and long-slit/multi-object spectroscopy (MOS). FORS2 was equipped with its red-sensitive MIT detector, a mosaic of two 2k×4k CCDs optimised for wavelengths longer than 6000 Å. In its standard resolution mode, the detector has a pixel size of 0.25" (2×2 binning) which corresponds to a field-of-view of 8.3'×8.3' over the CCD mosaic, although the effective sky coverage is lower due to vignetting. Observations were performed with the standard low gain, fast read-out mode and in high-resolution mode (0.125"/pixel) for PSR J1357-6429 and in standard resolution mode (0.25"/pixel) for PSR J1048-5832. Both targets were positioned in the upper CCD. Bright stars close to the PSR J1357-6429 position were masked using the MOS slitlets. Different filters were used: V (λ=5570 Å; Δλ=1235 Å), R (λ=6550 Å; Δλ=1650 Å), and I (λ=7680 Å; Δλ=1380 Å). To allow for cosmic ray removal and minimise saturation of bright stars in the field, sequences of short exposures (from 200 to 750 s) were obtained per each target and per each filter. The total integration time was 14700 s (V), 8800 s (R), and 1600 s (I) for PSR J1357-6429 and 24000 s (V) for PSR J1048-5832. Exposures were taken in dark time and photometric conditions, close to the zenith (airmass<1.3), and sub-arcsec image quality.

Data reduction

We reduced the data through standard packages in IRAF for bias subtraction, and flat-field correction using the closest-in-time bias and twilight flat-fields frames available in the ESO archive. Per each band, we aligned and average-stacked the reduced science images using the IRAF task drizzle applying a 3σ filter on the single pixel average to filter out residual hot and cold pixels and cosmic ray hits. Since all exposures have been taken with sub-arcsec image quality, we did not apply any selection prior to the image stacking. We applied the photometric calibration by using the extinction-corrected night zero points computed by the FORS2 pipeline and available through the instrument data quality control database (www.eso.org/qc).To register the pulsar positions on the FORS2 frames as precisely as possible, we re-computed their astrometric solution which is based on the coordinates of the guide star used for the telescope pointing. Since most stars from the GSC-2 are saturated in the stacked images, we used shorter exposures (10-15s) of the fields taken with the same instrument configurations. We measured the star centroids through Gaussian fitting using the GAIA tool and used the code ASTROM to compute the pixel-to-sky coordinate transformation though an high-order polynomial, which accounts for the CCD distortions. For both pulsar fields, the rms of the astrometry fits was ~0.1" in the radial direction. To this value we added in quadrature the uncertainty on the registration of the FORS2 image on the GSC2 reference frame (0.1") and the ~0.15" accuracy of the link of the GSC2 coordinates to the International Celestial Reference Frame (ICRF), we thus estimate that the overall (1σ) uncertainty of our FORS2 astrometry is ~0.2".

Astrometry

As a reference to compute the pulsar positions on the FORS2 frames we used their most recently published radio and Chandra coordinates (see Mignani et al. 2011). The radio and Chandra positions of PSR J1357-6429 and PSR J1048-5832 are shown in Fig. 1. For the former the Chandra position, averaged over multi-epoch consistent measurements, differs by 1.2"±0.4" from the radio interferometry one, an amount which can be explained by the ~7.2 yr time span between the epochs for a pulsar transverse velocity of 2100±700 km s^{-1}. For the latter, the difference between the Chandra and the radio-timing positions amounts to 4.1"±1.3" and cannot be explained by the pulsar proper motion between the two epochs (~5.4 yrs apart). However, the Chandra position is consistent with the radio-interferometry one, suggesting that the radio timing position was affected by timing noise. Since the multi-epoch Chandra coordinates appear more reliable, in the following we assume them as a reference, although we conservatively evaluate possible candidates at the radio positions.

Results and Discussion

The radio position of PSR J1357-6429 (Fig. 1, left) falls close (0.65") to a relatively bright field object (object A; V=21.8±0.06). We verified whether object A can be considered a possible counterpart to the pulsar. To quantitatively verify the significance of the association we measured the chance coincidence probability which turns out to be ~0.01, i.e. not statistically compelling yet. If it were its counterpart, the flux of object A would imply, after accounting for the uncertainties on the distance and interstellar extinction, an optical emission efficiency for PSR J1357-6429 up to 10 times larger than the Crab pulsar and up to ~5600 times larger than the Vela pulsar, to which it is more similar in its spin parameters. Thus, it is unlikely that object A is the pulsar counterpart.

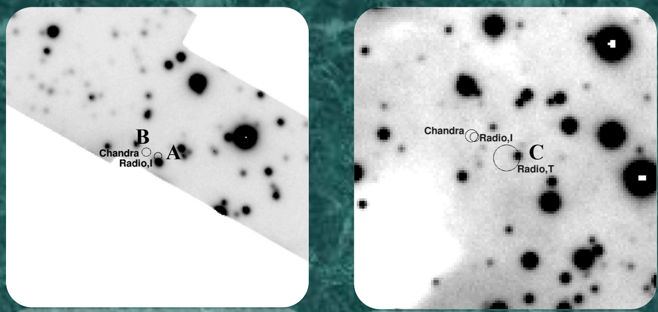

Fig.1. VLT/FORS2 observations of PSR J1357−6429 (left) and PSR J1048−5832 (right) taken in the V filter, with integration times of 14700 and 24000 s, respectively. North to the top, East to the left. Image cutouts are 30"×30" in size. The circles marks the pulsar radio (T=timing; I=interferometry) and Chandra positions.

To further test the association, we compared object A's colours (V=21.80±0.06; R=20.65±0.03; I=19.75±0.03) with those of field stars. The V-(V-R) and V-(V-I) colour-magnitude diagrams (CMDs) are shown in Fig. 2. As seen, object A's location is along the field sequence, i.e. it has no peculiar colours which may suggest its association with the pulsar. For instance, for a flat power-law spectrum, like that of the Vela pulsar, we would expect a (V-R)~0.2 and a (V-I)~0.1, once accounting for the interstellar extinction, which are obviously off the main sequence in both CMDs. Thus, we conclude that object A is unrelated to PSR J1357−6429. The same arguments also rule out object B (V=23.05±0.13; R=21.86±0.07; I=20.5±0.05) as a candidate counterpart.

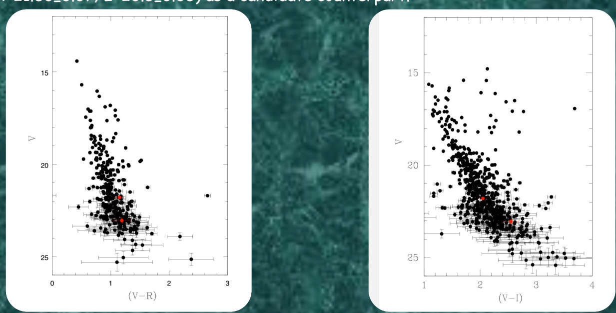

Fig.2: Observed (not extinction-corrected) colour-magnitude diagrams of the objects detected in the PSR J1357-6429 field. Objects A and B are marked in red.

The pulsar radio-timing position of PSR J1048-5832 (Fig. 1, right) falls close to a V~24 object (C). Again, the chance coincidence probability is ~0.04, i.e. certainly not low enough to statistically claim an association. This is also ruled out by the pulsar's energetics. The flux of object B would imply an optical emission efficiency for PSR J1048-5832 up to 60 times larger than the Crab pulsar and up to ~200000 times larger than the Vela pulsar. Thus, it is extremely unlikely that object B is associated with PSR J1048-5832.

No other possible counterparts are detected for PSR J1357-6429 and PSR J1048-5832 (Fig. 3). We conclude that both pulsars are unidentified in the VLT images and we computed the 3σ upper limits on the pulsar flux using the more robust Chandra positions as a reference. For PSR J1357-6429 we derive V>27.3, R>25.8, and I>25.2, while for PSR J1048-5832 we derived V>28. These upper limits suggest an efficiency in converting spin-down power into optical luminosity $<10^{-7}$ and $<10^{-6}$, respectively, lower than the Crab pulsar and, possibly, more compatible with the spin-down age of these two pulsars.

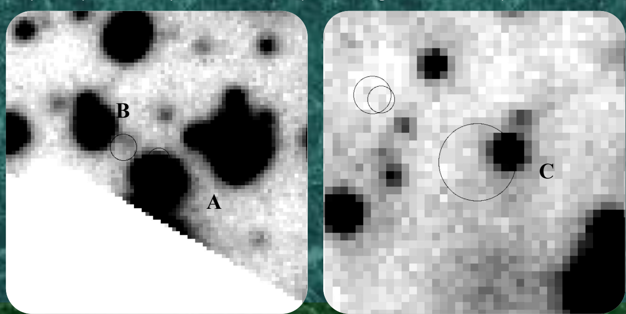

Fig.3: 10"x10" zoom around PSR J1357-6429 (left, I band) and PSR J1048-5832 (right, V band) . An excess of flux, undetected in the B and V bands, is noticed southwest of object B. It is unclear whether it is due to a background fluctuation or to a partially resolved object in the PSF of the two adjacent stars.

References

Mignani, R.P., 2011, AdSpR, 47,1281

Mignani, R.P., et al., 2011a, A&A, in preparation

Mignani, R.P., et al., 2011ab A&A, to be submitted

Shearer, A., & Golden, A., 2001, ApJ, 547, 967

Shearer, A., et al., 2010, in High Time Resolution Astrophysics IV, PoS, arXiv:1008.0605

Shearer, A., 2011, MNRAS, to be submitted